Tao Fulu (Orcid ID: 0000-0001-8574-0080)
Lall Upmanu (Orcid ID: 0000-0003-0529-8128)

Larger Drought and Flood Hazards and Adverse Impacts on Population and Economic Productivity under 2.0 than 1.5°C Warming

Ran Zhai[1,2], Fulu Tao[1,2,3*], Upmanu Lall[4,5], Bojie Fu[6], Joshua Elliott[7], Jonas Jägermeyr[7,8]

[1]Key Laboratory of Land Surface Pattern and Simulation, Institute of Geographic Sciences and Natural Resources Research, Chinese Academy of Sciences, Beijing 100101, China

[2]College of Resources and Environment, University of Chinese Academy of Sciences, Beijing 100049, China

[3]Natural Resources Institute Finland (Luke), 00790 Helsinki, Finland

[4]Columbia Water Center, Columbia University, New York 10027, USA

[5]Department of Earth and Environmental Engineering, Columbia University, New York 10025, USA

[6]State Key Laboratory of Urban and Regional Ecology, Research Center for Eco-Environmental Sciences, Chinese Academy of Sciences, Beijing 100085, China

[7]Department of Computer Science, University of Chicago, Chicago, IL 60637, USA

[8]NASA Goddard Institute for Space Studies, New York, NY 10025, USA.

*Correspondence: Fulu Tao (taofl@igsnrr.ac.cn)

Key Points:

- Annual runoff generally increases while terrestrial ecosystem water retention generally decreases under 2.0 than 1.5°C warming
- More areas would experience droughts (34.6%), floods (54.4%), droughts and floods (14.5%) under 2.0 than 1.5°C warming
- More people (85.9% totally) and GDP (85.9% totally) would be affected by droughts or/and floods under 2.0 than 1.5°C warming

This article has been accepted for publication and undergone full peer review but has not been through the copyediting, typesetting, pagination and proofreading process which may lead to differences between this version and the Version of Record. Please cite this article as doi: 10.1029/2019EF001398

Abstract

Climate change may have major influences on surface runoff, which would consequently result in important implications for terrestrial ecosystems and human well-being. At global scale there is limited understanding of these issues with respect to the warming targets stipulated in the Paris Agreement. Here we use a well-established hydrological model (Variable Infiltration Capacity; VIC) forced with a representative ensemble of latest climate projections from four global circulation models (GCMs) to estimate potential future changes in runoff and Terrestrial Ecosystem Water Retention (TEWR), as well as changes in extreme runoff and their impacts on population, and overall gross domestic product (GDP) worldwide. Results suggest that annual runoff generally would have larger increases, while annual TEWR generally would have larger decreases under the 2.0°C warming scenario as opposed to 1.5°C warming scenario. Global mean warming of 2°C versus 1.5°C would lead to more distinct spatial patterns in runoff change, with a general shift of the runoff distribution towards more extreme low runoff in Mexico, western U.S., Western Europe, southeastern China, West Siberian Plain and more extreme high runoff in Alaska, northern Canada, and large parts of Asia. More people and GDP would be exposed to extreme low runoff decrease, extreme high runoff increase, extreme low runoff decrease as well as extreme high runoff increase under a higher warming scenario. This study differentiates hydrological impacts between the two warming scenarios and illustrates higher runoff, lower TEWR, larger potential drought and flood hazards and adverse impacts on population and GDP under 2°C than 1.5°C.

1. Introduction

Climate impact assessments and associated adaptation strategies at regional and global scales have been a key concern for various sectors, such as water, agriculture, and ecosystem (Frieler et al., 2017; Prudhomme et al., 2014; Rosenzweig et al., 2014; Schewe et al., 2014). The Paris Agreement, produced by United Nations Framework Convention on Climate Change (UNFCCC, 2015), aims at holding the global mean temperature increase to well below 2.0°C compared to pre-industrial levels, which results in efforts to explore 1.5°C pathways (IPCC, 2018; Mitchell et al., 2017; Schleussner et al., 2016). Consequently, recent climate impact assessments largely focus on the differences between those two warming targets (Betts et al., 2018; Nangombe et al., 2018). Freshwater is vital for sustaining human activities and environmental requirements (Liu, Lim, et al., 2018). Global warming leads to changes in the distribution of water resources in many regions, and the global and regional hydrological cycles have been greatly influenced by climate change, and consequently leads to more frequent and more severe drought and flood hazards (Döll & Müller Schmied, 2012; Hagemann et al., 2013; Heinke et al., 2019; IPCC, 2018). With indispensable societal dependencies, freshwater is at the heart of climate impact assessments, but at the same time one of the most vulnerable sectors to climate change (Döll & Müller Schmied, 2012; Hagemann et al., 2013; Heinke et al., 2019; IPCC, 2018).

In addition, extreme weather events and associated low or high runoff levels have attracted wide attention recently (Dottori et al., 2018; Leng et al., 2016; Yin et al., 2018). With increasing global mean temperature, extreme precipitation is expected to intensify, which has been supported by both historical observations and model simulations (Asadieh & Krakauer, 2017; O'Gorman & Schneider, 2009; Trenberth, 2011). Shifts towards more intense precipitation may increase the severity and frequency of extreme runoff in different regions (Alfieri et al., 2015; Dankers et al., 2014), which is often directly associated with adverse impacts on human well-

being and economic status. Some previous studies have analyzed potential changes of droughts under different warming scenarios (Liu, Sun, et al., 2018; Liu, Lim, et al., 2018; Su et al., 2018). All of these have indicated that more droughts and floods would happen under warming scenarios, and consequently, more adverse impacts would happen under warming scenarios. On the contrary, there have been arguments that floods are decreasing despite of increases in extreme rainfall (Sharma et al., 2018) based on observed data, except in the most extremes cases, including small catchments or urban catchments (Wasko & Sharma, 2017), indicating precipitation change is not the only reason for flood change in the future.

Empirical approaches and process-based approaches have been used to investigate runoff change under warming scenarios in the future (Asadieh & Krakauer, 2017; Heinke et al., 2019; Liu, Sun, et al., 2018; Liu, Lim, et al., 2018; Su et al., 2018). Process-based approaches estimate runoff by describing various components of the hydrological cycle such as interception and evaporation. However, empirical-based approaches estimate runoff or droughts through quantifying patterns between observed hydrological indices and catchment characteristics without considering physical hydrological processes explicitly (Booker & Woods, 2014; Bourdin et al., 2012). Most climate change impact assessment studies are conducted at regional scale to quantify runoff change under warming scenarios (Kay et al., 2018; Leng et al., 2015; Leng et al., 2016; Zhai et al., 2018), while only a few studies have used process-based models at high spatial resolution and at global scale because of high computation cost (Asadieh & Krakauer, 2017; Heinke et al., 2019). Moreover, some global hydrological models are not enough calibrated for climate change impact assessment at a regional scale (Gosling et al., 2017). In addition, compared with the previously used climate change scenarios from Coupled Model Inter-comparison Project (CMIP), the climate change scenarios provided by "Half a degree Additional warming, Prognosis and Projected Impacts" (HAPPI) project are particularly designed for impact assessment in terms of Paris Agreement (Mitchell et al., 2016; Mitchell et

al., 2017).

Terrestrial ecosystem services have increasingly become concerned with global climate change. Terrestrial Ecosystem Water Retention (TEWR), representing water retained in terrestrial ecosystems, is one of important ecosystem services (Gong et al., 2017; Xu et al., 2017). There are some scattered case studies, but limited comprehensive assessments at a regional or global scale. TEWR is shown to increase in mainland China for the period of 2000-2010 because of natural capital investment policies, changes in biophysical factors, and socioeconomic development (Ouyang et al., 2016). However, how TEWR will be affected by global warming in the future has been rarely investigated.

Hazard represents the potential occurrence of a natural or human-induced physical event or trend or physical impact that may cause loss of life, injury, or other health impacts, as well as damage and loss to property, infrastructure, livelihoods, service provision, ecosystems, and environmental resources (IPCC, 2014). In this study, a decrease in extreme low runoff is associated with drought hazard, while an increase in extreme high runoff is associated with flood hazard (Asadieh & Krakauer, 2017). Climate change impacts on annual runoff and extreme runoff have been investigated previously, but the subsequent influences on socio-economy have been rarely investigated (Dottori et al., 2018). Population and GDP are key indicators of socio-economy development. Population and GDP would suffer directly from runoff change and especially extreme runoff change, such as water supply, navigation, hydropower generation, droughts and floods (Döll & Müller Schmied, 2012; Heinke et al., 2019). Therefore, in this study, we choose population and GDP to evaluate the adverse impacts of drought and flood hazards on socio-economy development.

We present one of the most comprehensive analyses targeting global runoff and TEWR change specifically differentiating the 1.5 and 2.0°C warming scenario. This analysis is based on the well-established hydrological model VIC with a worldwide spatial resolution of 0.5°.

We calibrate VIC at 18 major river basins (Table S1) before running it with 20 bias-corrected future climate projections from a rigorous selection of 4 representative GCMs: ECHAM6-3-LR, MIROC5, NorESM1-HAPPI, and CAM4-2degree (Table S2). This study aims to investigate (1) how annual runoff and TEWR will change; (2) how the extreme low and high runoff will change, and (3) how the projected changes in extreme runoff will affect population and GDP, under the 1.5 and 2.0°C warming scenarios, respectively. Based on previously studies (Dottori et al., 2018; Heinke et al., 2019; Liu, Sun, et al., 2018; Liu, Lim, et al., 2018), extreme low runoff is supposed to decrease while extreme high runoff to increase under warmer scenarios, which implies more droughts and floods and more adverse impacts on population and GDP with climate warming. We also assume that a well calibrated process-based hydrological model forced by dedicated climate change scenarios will produce more robust results.

2. Materials and Methods

2.1 Model description

The process-based model VIC (Liang et al., 1994, 1996) is applied for the hydrological modeling in this study. The model, developed for large-scale applications, considers different soil types and three layers, and dynamic natural vegetation growth in each grid cell. Here we run it at a 0.5° spatial grid with global coverage. In this study, VIC soil-related parameters such as soil texture and vegetation parameters within each grid, including number of vegetation classes, fraction of the grid covered by each vegetation, and root zone thickness as well as fraction of root in corresponding zones for every vegetation type, are introduced by Nijssen, Schnur, et al., (2001) and Nijssen, O'Donnell, et al., (2001) mainly based on FAO soil map (FAO 1995), World Inventory of Soil Emission Potentials (WISE) database (Batjes, 1995) and 1 km AVHRR-derived land cover data (Hansen et al., 2000). In each grid cell, up to 12 land

cover types are explicitly simulated, including evergreen needleleaf forests, evergreen broadleaf forests, deciduous needleleaf forests, deciduous broadleaf forests, mixed forests, woodlands, wooded grasslands/shrublands, closed shrublands, opened shrublands, grasslands, croplands and bare soil. Total evapotranspiration is separately calculated for each land cover type (*n*th) from canopy evaporation ($E_{c,n}$, mm) and vegetation transpiration ($E_{t,n}$, mm), and evaporation from the bare soil (E_1, mm). Total runoff consists of surface runoff ($Q_{s,n}$, mm) and base flow ($Q_{b,n}$, mm) (Liang et al., 1994). The VIC model uses the variable infiltration curve to account for the spatial heterogeneity of runoff generation. It assumes that surface runoff for the upper two soil layers is generated by those areas for which precipitation exceeds the storage capacity of the soil. The method of ARNO model (Todini, 1996) is used to describe base flow generation, which only happens in the bottom soil layer. A routing model is used to calculate runoff in each basin after running VIC model (Lohmann et al., 1996, 1998a, 1998b).

2.2 VIC model calibration and validation

There are seven parameters to be calibrated for the VIC model, including the variable infiltration curve parameter (b), the maximum velocity of base flow (D_{smax}), the fraction of D_{smax} where non-linear base flow begins (D_{s}), the fraction of maximum soil moisture where non-linear base flow occurs (W_{s}), and the thickness of each soil moisture layer (d_{i}, i=1, 2, 3). Historical daily climate data from the Water and Global Change (WATCH) project (Weedon et al., 2011) at a 0.5° spatial resolution are used for calibration and validation in the 18 river basins (Table S1). In this dataset, precipitation is corrected using Global Precipitation Climatology Centre full product (GPCC) version 4 and Climatic Research Unit (CRU) TS2.1 gridded observations, and temperature is corrected based on CRU TS2.1. Comparisons have shown a good agreement between WATCH forcing data and FLUXNET data at seven sites. The WATCH forcing data has been used widely (Dalin et al., 2012; Y. Liu et al., 2018; van Vliet et al., 2013).

The 18 major basins include Amazonas River basin (AMA), Amur River basin (AMU), Congo River basin (CON), Danube River basin (DAN), Ganges River basin (GAN), Lena River basin (LEN), Mackenzie River basin (MAC), Mekong River basin (MEK), Mississippi River basin (MIS), Murry River basin (MUR), Niger River basin (NIG), Nile River basin (NIL), Ob River basin (OB), Rio Parana River basin (PAR), Volga River basin (VOL), Yangtze River basin (YAN), Yellow River basin (YEL), Yenisey River basin (YEN). We calibrate model parameters individually for all the 18 river basins, at a spatial resolution of 1.0° instead of 0.5° to reduce computational costs for calibration. Previous studies have documented this calibration procedure at a higher spatial resolution does not significantly improve results (Haddeland et al., 2002; Zhou et al., 2016). Input data are aggregated to 1° × 1° grid and calibration is performed against monthly runoff observations from the Global Runoff Data Center (GRDC) for basins outside China, and from local water resources department for Yellow River basin and Yangtze River basin in China. The global river routing networks dataset at 1° × 1°, which is upscaled from finer resolutions using a dominant river tracing (DRT) algorithm (Wu et al., 2011), is used in the routing model. A global optimization method, shuffled complex evolution method developed at the University of Arizona (SCE-UA) (Duan et al., 1994), is used to calibrate the seven parameters of the VIC model through fitting the simulated runoff from the VIC model to the observed runoff at the corresponding hydrological station. The Kling-Gupta efficiency (KGE) (Gupta et al., 2009) value is used as the objective function, which represents the fit between the simulated and observed runoff in the process of calibration in each basin. Target values are calculated as follows:

$$\mathrm{KGE} = 1 - ED, \tag{1}$$

$$ED = \sqrt{(r-1)^2 + (\alpha-1)^2 + (\beta-1)^2}, \tag{2}$$

$$r = \frac{Cov_{so}}{\sigma_s \cdot \sigma_o}, \tag{3}$$

$$\alpha = \frac{\sigma_s}{\sigma_o}, \quad (4)$$

$$\beta = \frac{\mu_s}{\mu_o}, \quad (5)$$

where *ED* is the Euclidian distance from the ideal point, r, α, β represent the linear correlation coefficient, relative variability, bias between simulated values (χ_s) and observed values (χ_o), respectively. μ_s, μ_o represent means of χ_s, χ_o, and σ_s, σ_o represent standard deviations of χ_s, χ_o. Cov_{so} is the covariance between χ_s and χ_o. A good simulation result will have KGE close to 1.

2.3 Selection of representative ensembles from each GCM

To select subsets from the vast amount of available GCM ensembles, several envelope-based methods have been proposed (Cannon, 2015; Lutz et al., 2016) to create a representative subset that covers the full extent of all ensembles. Here we use the Katsavounidis-Kuo-Zhang (KKZ) method (Cannon, 2015; Chen et al., 2016; Katsavounidis et al., 1994; Wang et al., 2018) to select five representative ensembles in each GCM. The VIC model has four input variables, including daily precipitation (mm), mean wind speed (m/s), maximum (Tmax) and minimum (Tmin) temperature (°C). Mean values of these four input variables are calculated individually for each climate model ensemble (3 GCMs × 20 ensembles + 1 GCM × 10 ensembles; 70 ensembles in total) as grid-cell-area-weighted average for each continent, under the baseline period (2006-2015), as well as the 1.5 and 2.0°C warming scenarios (2106-2115). Respective relative changes in precipitation (ΔP/P, %) and wind speed (ΔWind/Wind, %), and absolute changes in maximum and minimum temperature ((ΔTmax+ΔTmin)/2, °C) at continental level are calculated. Changes are standardized to zero mean and unit standard deviation to eliminate influences from different magnitudes and units between variables. Finally, we select five

representative ensembles (Table S3) for each GCM through the following procedure: i) The ensemble closest to the centroid of all the ensembles is selected as the first representative ensemble; ii) The ensemble farest from the first selected ensemble is selected as the second representative ensemble; iii) The next three ensembles are selected according to their distance to previously-selected ensembles in that the distance to the nearest previously-selected ensemble is calculated. Then, the ensemble with the largest distance among the remaining ensembles is selected as the next representative ensemble.

2.4 Simulation protocol

Model simulations for the baseline (2006-2015) and future (2106-2115) for 1.5 and 2.0°C warming compared to pre-industrial conditions are forced by daily climate data obtained from the HAPPI project (Mitchell et al., 2017). For this climate forcing dataset, representative concentration pathway 2.6 (RCP2.6) are used to provide the model boundary conditions for the 1.5℃ warming scenario, and a weighted combination of RCP2.6 and RCP4.5 are used for the 2.0℃ warming scenario (Mitchell et al., 2017). Following the Inter-Sectoral Impact Model Intercomparison Project 2b (ISIMIP2b) (Frieler et al., 2017) simulation protocol, these model inputs have been bias-corrected using the trend-preserving bias correction method described in Hempel et al., (2013). The HAPPI input data are first interpolated to a 0.5°×0.5° grid, and then bias corrected using the EWEMBI (EartH2Observe, WFDEI and ERA-Interim data Merged and Bias-corrected for ISIMIP) dataset (Lange, 2018). Table S2 shows all considered ensemble members from each GCM. Then five ensembles are selected through KKZ method to decrease the computational cost for each warming scenario in every GCM. This results in 200 simulations (4 GCMs × 5 ensembles × 10 years) for each of the scenarios, respectively. Because there are only 10 years in every ensemble, so we repeat the first year for ten times as the spin-up period to make the model become stable, and then do simulations for the 10 years in each

ensemble of each scenario.

2.5 TEWR change

We calculate TEWR from a water balance perspective, that is, the ratio of input water and output water per grid cell, as follows:

$$\mathrm{TEWR} = \frac{P}{E+R}, \tag{6}$$

where P is precipitation (mm), ET is evapotranspiration (mm), and R is runoff (mm). TEWR is calculated at the monthly time scale and annual TEWR is the sum of monthly values.

2.6 Statistical analysis

Changes in annual mean temperature (°C), annual precipitation (%), annual runoff (%) and annual TEWR (%) in each grid are calculated in each ensemble for the future 10-year period (2106–2115) under 1.5 and 2.0°C warming scenarios relative to the baseline period. We adopt the median change (Tao & Zhang, 2011) among ensembles to represent the changing trend of every variable, including annual mean temperature, precipitation, runoff, and TEWR under the 1.5 and 2.0°C warming scenarios by ECHAM6-3-LR, MIROC5, NorESM1-HAPPI, CAM4-2degree, and all of them, relative to baseline scenario. Basin means are calculated by calculating area-weighted averages. Extreme low runoff is defined as the 5th percentiles of the consecutive 10-years mean 7-days runoff, and extreme high runoff is defined as the 95th percentiles of the consecutive 10-years daily runoff. Median changes among all ensembles (4 GCMs × 5 ensembles) are used to represent changes of extreme low and high runoff in each grid under 1.5 and 2.0°C warming scenarios, relative to baseline period.

The coefficient of determination (r^2) between each predictor to dependent variable is used to reveal driving factors that cause changes in runoff and TEWR from the 400 change samples in each grid cell (4 GCMs × 5 ensembles × 2 scenarios × 10 years). As for runoff, there are

four climate variables used in each simulation, including precipitation, maximum temperature, minimum temperature, and wind speed. Strong correlation exists between maximum and minimum temperature, so we analyze the effects of three climate variables, including annual precipitation change, annual mean temperature change, annual mean wind speed change on annual runoff change. The equation to calculate TEWR has three input variables, including precipitation, evapotranspiration, and runoff. So we analyze the effects of these three variables, including annual precipitation change, annual evapotranspiration change, and annual runoff change, on annual TEWR change. The weight of r^2 of each predictor to the sum of r^2 of the three predictors are calculated to represent the relative contribution of each variable in each grid, and defines a specific RGB color.

2.7 Impacts of extreme runoff change on population and GDP

To consider the number of people and GDP affected by runoff change, we use the historical and future population data and GDP data at a spatial resolution of 0.5° from the ISIMIP2b (Frieler et al., 2017). The shared socioeconomic pathways (SSPs) are scenarios of the GDP and population growth throughout the coming centuries. There are 5 SSPs designed to cover a broad range of future socioeconomic development pathways (O'Neill et al., 2017), including: SSP1 (Sustainability), SSP2 (Middle of the Road), SSP3 (Regional Rivalry), SSP4 (Inequality), SSP5 (Fossil-fueled Development). According to Döll et al. (2018), Frieler et al. (2017), Heinke et al. (2019) and Sun et al. (2019), the population and GDP data based on SSP2 projections are adopted in the future time period because the SSP2 describes a development pattern of moderate challenges to mitigation and adaptation (Fricko et al., 2017). In this study, global gridded population and GDP data in 2005 are used to represent population and GDP condition under baseline period (2006-2015), while global gridded population and GDP data in 2099 are used to represent population and GDP condition under 1.5 and 2.0°C warming

scenarios (2106-2115). Top 20 countries are selected according to population and GDP data in 2005, respectively (Table 1).

3. Results

3.1 VIC model parameters' calibration and validation

In this study, we first select top 10 basins according to length, surface area, total runoff, respectively, then add one more river basin in Europe and South America. Finally, 18 main river basins are selected (Figure S1), including CON, NIG and NIL in Africa, AMU, GAN, LEN, MEK, OB, YAN, YEL, YEN in Asia, DAN and VOL in Europe, MAC and MIS in North America, MUR in Oceania, AMA and PAR in South America. Summary characteristics of each basin, including location and area, are shown in the Table S1. The calibration period is about 10 years (mostly from 1980 to 1989) in each basin, and validation period range from 1990 to 1999 in most basins (Table S1). The calibrated VIC model simulates runoff fairly well in most main basins (Figure 1). In 14 out of 18 basins, the KGE value exceeds 0.5 in both the calibration and validation period. The four basins in which the model does not perform well, with the KGE value less than 0.5 in the calibration period and (or) in the validation period, include MUR, NIG, NIL, and YEL (Figure 1). This can be explained by the fact that channel losses in the routing process are not calculated (Nijssen, O'Donnell, et al., 2001), and the impact of human activities such as water withdrawal are not considered in this model. Despite these typical global model limitations, the calibration has improved simulation results in all basins. Since we only calibrate parameters in the 18 main basins in the world, the parameters of uncalibrated grids are set the same with the parameters of the calibrated nearest grid in the same continent.

3.2 Changes in runoff under 1.5 and 2.0°C warming scenarios and the controlling factors

Spatial-temporal changes in annual mean temperature and annual precipitation under 1.5 and 2.0°C warming scenarios (2106-2115), relative to baseline period (2006-2015), are shown

in Figure S2 and Figure S3. In general, the projected spatial patterns of runoff change are consistent with those of precipitation, suggesting runoff change should be dominated by precipitation change (Figure 2 and Figure S3), while the magnitude of the runoff change (%) is greater than the magnitude of the precipitation change (%). The annual runoff is projected to decrease in large areas in South America, Africa, Oceania and part of North America, Europe, and Asia under 1.5 °C warming scenario (Figure 2e). From 1.5 to 2.0°C warming scenario, runoff is projected to decrease in less grids located in South America, Africa, and Oceania, but in more grids located in the middle and low latitudes in North America, large parts in Europe and West Asia (Figure 2j). Generally, runoff is projected to increase more or decrease less under 2.0 than 1.5°C warming scenario. Runoff is projected to increase in 53.1% and 53.7% of the grids, while decrease in 30.6% and 30.0% of the grids, respectively, under 1.5 and 2.0°C warming scenarios. At the basin scale, annual runoff in seven (six) out of 18 basins are projected to decrease under 1.5°C (2.0°C) warming scenario (Table S4 and Figure S4c). Although annual runoff increases more (or decreases less) in large areas under 2.0 than 1.5°C warming scenario (Figure 2e,j and Figure S4c), it is projected to increase less (or decrease more) under 2.0 than 1.5°C warming scenario in some basins including the DAN, MIS, VOL, YAN, and YEL (Table S4 and Figure S4c). Annual runoff in the above-mentioned basins would change by -1.4% (-2.5%), 1.6% (-13.3%), 12.6% (4.5%), 10.0% (2.8%), and 12.0% (2.4%) under 1.5°C (2.0°C) warming scenario, respectively. We further investigate the factors controlling runoff change under the two warming scenarios (Figure 3). It is obvious that precipitation change is the major factor for runoff change over the world, however, temperature change and wind speed change influence runoff change through influencing evapotranspiration (Ekness & Randhir, 2015; She et al., 2017). In the VIC model, temperature and wind speed change influence runoff more in low latitudes of the Northern Hemisphere and in the Southern Hemisphere than middle and high latitudes of the Northern Hemisphere.

3.3 Changes in TEWR under 1.5 and 2.0°C warming scenarios and the controlling factors

The projected changes in TEWR (Figure 4) are less than those of precipitation and runoff (Figure S3 and Figure 2). Annual TEWR is projected to increase in large parts of Alaska, Canada, Russian Federation, Kazakhstan, Belarus, Ukraine, Pakistan under 1.5°C warming scenario (Figure 4e). It is projected to increase in large parts of Alaska, Canada, Russian Federation, Kazakhstan, Saudi Arabia under 2.0°C warming scenario (Figure 4j). In other parts of the world, TEWR is mainly projected to decrease or remain unchanged (Figure 4e,j). In 39.6% and 46.3% of the grids, it is projected to decrease under 1.5 and 2.0°C warming scenarios, while in 44.1% and 37.4% of the grids, it is projected to increase under 1.5 and 2.0°C warming scenarios. Generally, it is projected to decrease more (or increase less) under 2.0°C than 1.5°C warming scenario. At basin scale, compared with median changes in annual precipitation and runoff, median change in annual TEWR is projected to decrease in more basins (Table S4 and Figure S4d) under the two warming scenarios. Median change in annual TEWR in 8 out of 18 basins (including AMA, CON, GAN, MEK, MIS, MUR, VOL, YEL) is projected to decrease under 1.5°C warming scenario, and the decreasing trend is projected in 12 basins (including AMA, CON, DAN, GAN, MAC, MEK, MUR, NIL, PAR, VOL, YAN, YEL) under 2.0°C warming scenario. TEWR in 11 out of 18 basins (including AMA, AMU, DAN, GAN, MAC, MUR, NIG, NIL, PAR, YAN, YEN) is projected to decrease under 2.0 than 1.5°C warming scenario (Table S4 and Figure S4d). Increasing evapotranspiration accompanied with increasing temperature would lead to TEWR decrease to some extent. The controlling factors are investigated separately in this study (Figure 5). TEWR change is the result of multiple factors interactions, including climate conditions, terrain, soil texture, and land cover. For example, in northern Canada, Alaska, eastern United States, West Siberian Plain, East European Plain, and large areas in China and Mongolia, runoff change is the main factor controlling TEWR change.

3.4 Changes in extreme runoff under 1.5 and 2.0°C warming scenarios

Changes in extreme low and high runoff are investigated (Figure 6). Extreme low runoff is projected to decrease in 33.4% of grids over the world, mainly in South America, Africa, Southeast Asia, Central Europe and Southern Europe under 1.5°C warming scenario, which represents more drought hazards would exist in these areas (Figure 6a). When the warming target is 2.0°C instead of 1.5°C, extreme low runoff is projected to decrease in more grids (34.6%). Drought hazards are projected to decrease in South America, Africa and Central Europe under 2.0℃ than 1.5℃ warming, while they are projected to increase in Mexico, western U. S., Western Europe, southeastern China and West Siberian Plain (Figure 6b). Mean extreme low runoff is projected to decrease from -2.9% to -3.3% from 1.5 to 2.0°C warming scenarios. This means extreme low runoff is projected to decrease in more grids, and extreme low runoff is projected to decrease more under 2.0 than 1.5°C warming scenario. Extreme high runoff is projected to increase in 52.0% of grids over the world under 1.5°C warming scenario, which are mainly located in the Northern Hemisphere including southern U.S., Alaska, northern Canada, large parts of Asia, Northern Europe and areas in Africa near the equator (Figure 6c). Extreme high runoff is projected to increase in 54.4% of grids under 2.0°C warming scenario. More extreme high runoff is projected to increase in Alaska, northern Canada, large parts of Asia under 2.0 than 1.5°C warming scenario (Figure 6c,d). And the increase in extreme high runoff is significantly greater in 2.0°C warming scenario than 1.5°C warming scenario. Increase of mean extreme high runoff change is 4.5% and 6.5% under 1.5 and 2.0°C warming scenarios, respectively. Thus, more droughts and floods would happen under 2.0°C than 1.5°C warming. In addition, extreme high runoff is projected to increase, as well as extreme low runoff is projected to decrease concurrently in 12.8% and 14.5% of grids over the world under 1.5 and 2.0°C warming scenarios, which represents more droughts and floods would happen concurrently when global warming target increases from 1.5°C to 2.0°C.

3.5 Adverse impacts on population and GDP

The impacts of extreme runoff changes under warming scenarios on population and GDP are further analyzed. Total number of people is projected to increase from 6.5 billion in 2005 to 9.0 billion in 2099. However, total GDP is projected to increase nearly tenfold, from 59 to 532 trillion in 2005 PPP USD, during the period from 2005 to 2099. Three zones are defined according to extreme runoff change, including extreme low runoff decrease, extreme high runoff increase, extreme low runoff decrease as well as extreme high runoff increase. Percentage of population and GDP influenced by extreme runoff change in each zone are shown in Table 2 and Table 3. At the global scale, 44.6% (45.1%) of population would be influenced by extreme low runoff decrease, 56.1% (61.0%) of population would be influenced by extreme high runoff increase under 1.5°C (2.0°C) warming scenario. Therefore, more population would be influenced by droughts and floods under 2.0°C than 1.5°C warming. 15.3% (20.2%) of population would be influenced concurrently by extreme low runoff decrease and extreme high runoff increase under 1.5°C (2.0°C) warming scenarios, which means more population would be influenced by droughts and floods simultaneously with global warming of 2.0°C than 1.5°C (Table 2). 43.7% and 57.1% of GDP would be influenced by extreme low runoff decrease and extreme high runoff increase under 1.5°C warming scenario, respectively. These percentage increased to 48.3% and 59.5% under 2.0°C warming scenario, respectively. Same as population, the percentage of GDP influenced by both decrease in extreme low runoff and increase in extreme high runoff would increase from 16.2% to 21.9% with global warming of 1.5°C to 2.0°C (Table 3). More people and GDP would experience adverse impacts of droughts and floods from 1.5 to 2.0°C warming scenario. Therefore, limiting global average temperature increase to below 1.5 instead of 2.0°C warmer than pre-industrial levels would reduce the percentage of population and GDP influenced by droughts and floods.

Runoff change has an obvious spatial heterogeneity. Population and GDP in each grid

414 which would be influenced in different runoff change zones under 1.5 and 2.0°C warming
415 scenarios are shown in Figure S5 and Figure S6. Grids with high population density (>200,000)
416 influenced by extreme low runoff decrease are mainly located in Sub-Saharan Africa, Western
417 Europe, Central Europe, Southern Europe, Central America, northern South America, eastern
418 U.S., South Asia, southeastern China, and Southeast Asia under 1.5 and 2.0°C warming
419 scenarios (Figure S5a,d). The number of such grids would increase notably in southeastern
420 China under 2.0 than 1.5°C warming scenario (Figure S5a,d). The grids with high population
421 density influenced by extreme high runoff increase are mainly located in India, East Asia,
422 Southeast Asia, Western Africa, western Central Africa, Central Europe under 1.5°C warming
423 scenario (Figure S5b). When global warming increases from 1.5°C to 2.0°C, besides above-
424 mentioned areas, the grids in Eastern Africa also have a large population influenced by extreme
425 high runoff increase (Figure S5e). The grids with a high population density influenced by both
426 extreme low runoff decrease and extreme high runoff increase are mainly scattered in South
427 Asia, East Asia, and Southeast Asia, under 1.5°C warming scenario. And these grids are mainly
428 scattered in Western Africa, Eastern Africa, Central Europe, South Asia, East Asia, and
429 Southeast Asia under 2.0°C warming scenario (Figure S5c,f). The GDP affected by extreme
430 runoff change have nearly the same spatial pattern as population under both 1.5 and 2.0°C
431 warming scenarios (Figure S6).

432 The top 20 countries are selected according to the population and GDP data in 2005,
433 respectively (Table 1). The affected population and GDP in grids, which are suffered from
434 extreme low runoff decrease, extreme high runoff increase, extreme low runoff decrease as
435 well as extreme high runoff increase, are summed in each country. Then the ratios of affected
436 population (GDP) to all population (GDP) in these 20 countries under 1.5 and 2.0°C warming
437 scenarios are calculated (Figure 7). The percentage of population would be more influenced by
438 floods (extreme high runoff increase) than droughts (extreme low runoff decrease) in China,

India, Russian Federation, Nigeria, Bangladesh, Japan, Philippines, Viet Nam, Egypt, Iran, and Thailand under the two warming scenarios. As for United States of America, Indonesia, Brazil, Pakistan, Mexico, Turkey, and France, the percentage of population would be more influenced by droughts than floods under the two warming scenarios (Figure 7a). Percentage of GDP would be more influenced by floods than droughts in China, Japan, India, Russian Federation, Korea (the Republic of), Iran, and Saudi Arabia. By contrast, it would be more influenced by droughts than floods in France, Italy, Brazil, Mexico, Spain, Canada, Indonesia, Turkey, and Australia (Figure 7b). Obviously, the population and GDP in most of the selected countries in Asia would be influenced by floods. More than 30% of population in Philippines (China, Indonesia, Pakistan, Germany) are projected to be affected by droughts and floods concurrently under 1.5°C (2.0°C) warming scenario (Figure 7a). More than 30% of GDP in Italy and Korea (the Republic of) (China, Germany, United Kingdom of Great Britain and Northern Ireland, Indonesia) are projected to be affected by droughts and floods concurrently under 1.5°C (2.0°C) warming scenario (Figure 7b).

4. Discussion

4.1 Larger drought and flood hazards and adverse impacts on population and economic productivity under 2.0 than 1.5°C warming

Future runoff changes under warming scenarios have been investigated using different methods under various warming scenarios (Hagemann et al., 2013; Krysanova et al., 2017; Milly et al., 2005). In recent years, extreme runoff including droughts and floods has been investigated more frequently, with different evaluation criteria varying from daily, monthly to yearly to account for changes in extreme runoff (Gosling et al., 2017; Henley et al., 2019; Zhai et al., 2018). The results show that more land areas would be exposed to potential flood hazards than drought hazards, which is supported by other studies using different GCMs and hydrological models under RCP2.6 scenario (Asadieh & Krakauer, 2017). Liu, Lim, et al., (2018) used a mathematical approach combined with HAPPI climate scenarios to quantify changes in the magnitude of monthly water availability below normal conditions. Their results showed that more (less) people in East Asia, Central Europe, South Asia, and Southeast Asia (Western Africa and Alaska/northwestern Canada) would be exposed to water shortage. Their results have some differences from this present study due to use of different droughts indicators, and study methods (process-based hydrological model vs mathematical approach). Dottori et al., (2018) investigated flooding impacts using the ISIMIP fast-track multi-model hydrological ensemble and found the greatest losses would happen in the Asian continent at 1.5°C, 2.0°C, and 3.0°C warming scenarios. In addition, there are some studies at global or regional scale, showing that global warming would lead to more floods, more droughts, and more adverse impacts on population and GDP, albeit with some differences (Gosling et al., 2017; Heinke et al., 2019; Liu, Sun, et al., 2018). Compared with the previous studies, we use a well calibrated process-based hydrological model forced by 20 representative climate projections to investigate annual mean runoff, annual mean TEWR, droughts and floods, as well as the

adverse impacts on population and GDP, aiming to provide more comprehensive, systematic and robust results. The findings presented in this study supplement the climate change impact assessment on runoff change forced by earlier climate modeling archives, such as CMIP5, especially for the global warming target put forward by the Paris Agreement.

4.2 Representativeness of selected climate projections

Although it is always advised to use all available climate projections in impact studies, the cost of storage and computation may be prohibitive (Wang et al., 2018). Therefore, we use KKZ method to select five representative climate projection ensembles from each GCM (Table S3). The representativeness of selected ensembles is first analyzed at continental scale. For each continent under the two warming scenarios, the absolute values of difference between the median value of 20 selected ensembles and the median value of all 70 ensembles are no more than 1.52%, 0.12℃, 0.09℃, and 0.52%, respectively, for changing in area-weighted mean of daily precipitation, maximum temperature, minimum temperature, and wind speed under the two warming scenarios (Figure 8). Percentage of spread coverage (PSC) is calculated by dividing the variable's range in the selected ensembles by the variable's range in all ensembles. PSC is no less than 74.81% for changes of all the four variables in the two warming scenarios at continental scale (Figure 8). At grid scale, the absolute values of differences between the median values of the 20 selected ensembles and median values of all the 70 ensembles in 80% grids are less than 2.76%, 0.14℃, 0.12℃, and 1.06%, respectively, for precipitation, maximum temperature, minimum temperature, and wind speed change under the two warming scenarios (Figure S7). PSC for 80% of grids are more than 63.79%, 72.51%, 73.72%, and 70.72%, respectively, for changes in precipitation, maximum temperature, minimum temperature, and wind speed for the selected ensembles (Figure S8). Therefore, the selected ensembles through KKZ method are able to reduce the computational cost while representing the median values

of changes and the uncertainties of all ensembles.

4.3 Uncertainties and limitations

There may exist some uncertainties from future projections in climate change, population, and GDP (Allen et al., 2000; Woldemeskel et al., 2014). In this study, we try to account for the climate model uncertainties by using a large number of ensembles. Nevertheless, it's worth noting that HAPPI samples a recent decade and then uses low RCP scenarios to produce the Paris Agreement warmer worlds. This means that it is only sampling aspects of interannual climate variability in the recent climate and cannot project changes in sea surface temperatures (SST) variability that may occur, for example more frequent El Niño or La Niña events (Cai et al., 2015, 2018). The projections in affected number of people and GDP under warming scenarios can be dependent on the selection of SSP scenario and the definition of drought and flood hazards (Döll et al., 2018; Heinke et al., 2019; Liu, Sun, et al., 2018). If we use the projections of population and GDP under SSP1 scenario, the projections in affected number of people and GDP by droughts and floods may be less compared with SSP2 scenario. The WATCH forcing data is applied to provide climate forcing data but there is observational uncertainty (Herold et al., 2016) that is not captured by the use of one dataset alone. The robustness of the results could be further confirmed using other forcing datasets, since the simulated results are strongly affected by the uncertainty in the climate forcing data (Müller Schmied et al., 2016; Herold et al., 2016). The land cover are assumed constant in hydrological model integrations lead to a systematic bias since global warming as well as projected potential increases in droughts or floods would likely lead to land cover change, which in turn lead to runoff change (Li et al., 2018; Piao et al., 2007). And human activities also have unavoidable impacts on water resources (Huang et al., 2018). Urbanization may have increased floods caused by larger proportion of impermeable surfaces, while construction of dams may have

opposite effect caused by more regulation (Wasko & Sharma, 2017). Precipitation change is not the only reason for flood change. Uncertainty remains in the relationships between changes in precipitation and flood magnitude across the spectrum of catchment, storm, and antecedent hydrologic conditions (Sharma et al., 2018). Furthermore, projected increases in droughts or floods, may lead to either the increase in mortality rate in those areas, or immigration to more suitable areas, which are not taken into accounted in the population data (Heinke et al., 2019). These are limitations associated with nearly all future predictions and are worth to investigate in further studies.

5. Conclusions

In this study, we provide a comprehensive and systematic assessment of runoff change, TEWR change, extreme low and high runoff change and the adverse impacts on population and GDP under 1.5 and 2.0°C warming scenarios through a well-established hydrological model VIC. Hazards and adverse impacts are projected to increase under 2.0 than 1.5°C warming scenario. Annual runoff is projected to increase more under 2.0 than 1.5°C warming scenario. Annual TEWR is projected to decrease more under 2.0 than 1.5°C warming scenario. Similar to our hypotheses, more potential droughts and floods are projected under 2.0 than 1.5°C warming scenario. Potential drought hazards are projected to happen in large parts of the Southern Hemisphere, Southern Europe. And potential flood hazards are projected to happen in many areas in Asia and the northern part of North America under the two warming scenarios. About 44.6% (45.1%), 56.1% (61.0%), 15.3% (20.2%) of population is projected to be affected by droughts, floods, droughts and floods concurrently under 1.5°C (2.0°C) warming scenario. Similarly, about 43.7% (48.3%), 57.1% (59.5%), 16.2% (21.9%) of GDP is projected to be affected by droughts, floods, droughts and floods concurrently under 1.5°C (2.0°C) warming scenario. Our results identify the vulnerable regions where should be put more efforts in mitigating hazards of drought and flood over the world. Drought and flood hazards would

probably happen in some areas with high density of population and GDP, including Sub-Saharan Africa, Southern Europe, Central Europe, Western Europe, South Asia, Southeast Asia, East Asia, Central America, and eastern U.S. under the 1.5 and 2.0°C warming scenarios. Societal impacts on main countries in Asia would be mainly associated with floods. The study highlights the need for governments around the world to pursue efforts to limit the global warming to 1.5°C.

Acknowledgements

Climate projections from HAPPI data are available at http://portal.nersc.gov/c20c/data/ClimateAnalytics/. Observed runoff data and the boundaries of the eighteen main basins are available at https://www.bafg.de/GRDC/EN/Home/homepage_node.html. Global VIC input data at 0.5-degree resolution are available at https://vic.readthedocs.io/en/master/Datasets/Datasets/. Global River Routing Networks at 1-degree are obtained at https://vic.readthedocs.io/en/master/Datasets/Datasets/. We acknowledge the HAPPI core team and NERSC for data storage. We acknowledge ISIMIP for providing population data, GDP data and WATCH climate data at a 0.5° resolution. Supplementary Information is available online. The authors declare no competing financial interests. This work was supported by the National Key Research and Development Program of China (no. 2017YFA0604703) and the National Natural Science Foundation of China (nos. 41571088, 41571493, and 31561143003). R.Z. acknowledges financial support from China Scholarship Council.

Reference

Alfieri, L., Burek, P., Feyen, L., & Forzieri, G. (2015). Global warming increases the frequency of river floods in Europe. *Hydrology and Earth System Sciences*, *19*(5), 2247-2260. http://doi.org/10.5194/hess-19-2247-2015

Allen, M. R., Stott, P. A., Mitchell, J. F. B., Schnur, R., & Delworth, T. L. (2000). Quantifying the uncertainty in forecasts of anthropogenic climate change. *Nature*, *407*(6804), 617-620. http://doi.org/10.1038/35036559

Asadieh, B., & Krakauer, N. Y. (2017). Global change in streamflow extremes under climate change over the 21st century. *Hydrology and Earth System Sciences*, *21*(11), 5863-5874. http://doi.org/10.5194/hess-21-5863-2017

Batjes, N. H. (1995). A homogenized soil data file for global environmental research: A subset of FAO, ISRIC and NRCS profiles (Version 1.0), ISRIC, Wageningen.

Betts, R. A., Alfieri, L., Bradshaw, C., Caesar, J., Feyen, L., Friedlingstein, P., et al. (2018). Changes in climate extremes, fresh water availability and vulnerability to food insecurity projected at 1.5°C and 2°C global warming with a higher-resolution global climate model. *Philosophical Transactions of the Royal Society a-Mathematical Physical and Engineering Sciences*, *376*(2119), 20160452. http://doi.org/10.1098/rsta.2016.0452

Booker, D. J., & Woods, R. A. (2014). Comparing and combining physically-based and empirically-based approaches for estimating the hydrology of ungauged catchments. *Journal of Hydrology*, *508*, 227-239. http://doi.org/10.1016/j.jhydrol.2013.11.007

Bourdin, D. R., Fleming, S. W., & Stull, R. B. (2012). Streamflow Modelling: A Primer on Applications, Approaches and Challenges. *Atmosphere-Ocean*, *50*(4), 507-536. http://doi.org/10.1080/07055900.2012.734276

Cai, W. J., Wang, G. J., Dewitte, B., Wu, L. X., Santoso, A., Takahashi, K., et al. (2018). Increased variability of eastern Pacific El Niño under greenhouse warming. *Nature*, *564*(7735), 201-206. http://doi.org/10.1038/s41586-018-0776-9

Cai, W. J., Wang, G. J., Santoso, A., McPhaden, M. J., Wu, L. X., Jin, F. F., et al. (2015). Increased frequency of extreme La Niña events under greenhouse warming. *Nature Climate Change*, *5*(2), 132-137.

http://doi.org/10.1038/nclimate2492

Cannon, A. J. (2015). Selecting GCM Scenarios that Span the Range of Changes in a Multimodel Ensemble: Application to CMIP5 Climate Extremes Indices. *Journal of Climate*, *28*(3), 1260-1267. http://doi.org/10.1175/jcli-d-14-00636.1

Chen, J., Brissette, F. P., & Lucas-Picher, P. (2016). Transferability of optimally-selected climate models in the quantification of climate change impacts on hydrology. *Climate Dynamics*, *47*(9-10), 3359-3372. http://doi.org/10.1007/s00382-016-3030-x

Döll, P., & Müller Schmied, H. (2012). How is the impact of climate change on river flow regimes related to the impact on mean annual runoff? A global-scale analysis. *Environmental Research Letters*, *7*(1), 014037. http://doi.org/10.1088/1748-9326/7/1/014037

Döll, P., Trautmann, T., Gerten, D., Müller Schmied, H., Ostberg, S., Saaed, F., & Schleussner, C.-F. (2018). Risks for the global freshwater system at 1.5°C and 2°C global warming. *Environmental Research Letters*, *13*(4), 044038. http://doi.org/10.1088/1748-9326/aab792

Dalin, C., Konar, M., Hanasaki, N., Rinaldo, A., & Rodriguez-Iturbe, I. (2012). Evolution of the global virtual water trade network. *Proceedings of the National Academy of Sciences of the United States of America*, *109*(16), 5989-5994. http://doi.org/10.1073/pnas.1203176109

Dankers, R., Arnell, N. W., Clark, D. B., Falloon, P. D., Fekete, B. M., Gosling, S. N., et al. (2014). First look at changes in flood hazard in the Inter-Sectoral Impact Model Intercomparison Project ensemble. *Proceedings of the National Academy of Sciences of the United States of America*, *111*(9), 3257-3261. http://doi.org/10.1073/pnas.1302078110

Dottori, F., Szewczyk, W., Ciscar, J.-C., Zhao, F., Alfieri, L., Hirabayashi, Y., et al. (2018). Increased human and economic losses from river flooding with anthropogenic warming. *Nature Climate Change*, *8*(9), 781-786. http://doi.org/10.1038/s41558-018-0257-z

Duan, Q. Y., Sorooshian, S., & Gupta, V. K. (1994). Optimal use of the SCE-UA global optimization method for calibrating watershed models. *Journal of Hydrology*, *158*(3-4), 265-284. http://doi.org/10.1016/0022-1694(94)90057-4

Ekness, P., & Randhir, T. O. (2015). Effect of climate and land cover changes on watershed runoff: A multivariate assessment for storm water management. *Journal of Geophysical Research-Biogeosciences*, *120*(9), 1785-1796. http://doi.org/10.1002/2015jg002981

Fricko, O., Havlik, P., Rogelj, J., Klimont, Z., Gusti, M., Johnson, N., et al. (2017). The marker quantification of the Shared Socioeconomic Pathway 2: A middle-of-the-road scenario for the 21st century. *Global Environmental Change-Human and Policy Dimensions*, *42*, 251-267. http://doi.org/10.1016/j.gloenvcha.2016.06.004

Frieler, K., Lange, S., Piontek, F., Reyer, C. P. O., Schewe, J., Warszawski, L., et al. (2017). Assessing the impacts of 1.5°C global warming - simulation protocol of the Inter-Sectoral Impact Model Intercomparison Project (ISIMIP2b). *Geoscientific Model Development*, *10*(12), 4321-4345. http://doi.org/10.5194/gmd-10-4321-2017

Gong, S. H., Xiao, Y., Xiao, Y., Zhang, L., & Ouyang, Z. Y. (2017). Driving forces and their effects on water conservation services in forest ecosystems in China. *Chinese Geographical Science*, *27*(2), 216-228. http://doi.org/10.1007/s11769-017-0860-3

Gosling, S. N., Zaherpour, J., Mount, N. J., Hattermann, F. F., Dankers, R., Arheimer, B., et al. (2017). A comparison of changes in river runoff from multiple global and catchment-scale hydrological models under global warming scenarios of 1°C, 2°C and 3°C. *Climatic Change*, *141*(3), 577-595. http://doi.org/10.1007/s10584-016-1773-3

Gupta, H. V., Kling, H., Yilmaz, K. K., & Martinez, G. F. (2009). Decomposition of the mean squared error and NSE performance criteria: Implications for improving hydrological modelling. *Journal of Hydrology*, *377*(1-2), 80-91. http://doi.org/10.1016/j.jhydrol.2009.08.003

Haddeland, I., Matheussen, B. V., & Lettenmaier, D. P. (2002). Influence of spatial resolution on simulated streamflow in a macroscale hydrologic model. *Water Resources Research*, *38*(7), 1124. http://doi.org/10.1029/2001wr000854

Hagemann, S., Chen, C., Clark, D. B., Folwell, S., Gosling, S. N., Haddeland, I., et al. (2013). Climate change impact on available water resources obtained using multiple global climate and hydrology models. *Earth System Dynamics*, *4*(1), 129-144. http://doi.org/10.5194/esd-4-129-2013

Hansen, M. C., Defries, R. S., Townshend, J. R. G., & Sohlberg, R. (2000). Global land cover classification at 1km spatial resolution using a classification tree approach. *International Journal of Remote Sensing*, *21*(6-7), 1331-1364. http://doi.org/10.1080/014311600210209

Heinke, J., Müller, C., Lannerstad, M., Gerten, D., & Lucht, W. (2019). Freshwater resources under success and failure of the Paris climate agreement. *Earth System Dynamics*, *10*(2), 205-217.

http://doi.org/10.5194/esd-10-205-2019

Hempel, S., Frieler, K., Warszawski, L., Schewe, J., & Piontek, F. (2013). A trend-preserving bias correction - the ISI-MIP approach. *Earth System Dynamics*, *4*(2), 219-236. http://doi.org/10.5194/esd-4-219-2013

Henley, B. J., Peel, M. C., Nathan, R., King, A. D., Ukkola, A. M., Karoly, D. J., & Tan, K. S. (2019). Amplification of risks to water supply at 1.5°C and 2°C in drying climates: a case study for Melbourne, Australia. *Environmental Research Letters*, 14(8), 084028. http://doi.org/10.1088/1748-9326/ab26ef

Herold, N., Alexander, L. V., Donat, M. G., Contractor, S., & Becker, A. (2016). How much does it rain over land? *Geophysical Research Letters*, *43*(1), 341-348. http://doi.org/10.1002/2015gl066615

Huang, Z., Hejazi, M., Li, X., Tang, Q., Vernon, C., Leng, G., et al. (2018). Reconstruction of global gridded monthly sectoral water withdrawals for 1971-2010 and analysis of their spatiotemporal patterns. *Hydrology and Earth System Sciences*, *22*(4), 2117-2133. http://doi.org/10.5194/hess-22-2117-2018

IPCC (2014). In Field, C.B., Barros, V.R., Dokken, D.J., Mach, K.J., Mastrandrea, M.D., Bilir, T.E., Chatterjee, M., Ebi, K.L., Estrada, Y.O., Genova, R.C., Girma, B., Kissel, E.S., Levy, A.N., MacCracken, S., Mastrandrea, P.R., & White, L.L. (Eds.), Climate Change 2014: Impacts, Adaptation, and Vulnerability. Part A: Global and Sectoral Aspects. Contribution of Working Group II to the Fifth Assessment Report of the Intergovernmental Panel on Climate Change. Cambridge, United Kingdom and New York, NY, USA: Cambridge University Press.

IPCC (2018). In Masson-Delmotte, V., Zhai, P., Pörtner, H. O., Roberts, D., Skea, J., Shukla, P. R., Pirani, A., Moufouma-Okia, W., Péan, C., Pidcock, R., Connors, S., Matthews, J. B. R., Chen, Y., Zhou, X., Gomis, M. I., Lonnoy, E., Maycock, T., Tignor, M., & Waterfield, T. (Eds.), Global warming of 1.5°C. An IPCC Special Report on the impacts of global warming of 1.5°C above pre-industrial levels and related global greenhouse gas emission pathways, in the context of strengthening the global response to the threat of climate change, sustainable development, and efforts to eradicate poverty. Geneva, Switzerland: World Meteorological Organization.

Katsavounidis, I., Kuo, C.-C. J., & Zhang, Z. (1994). A New Initialization Technique for Generalized Lloyd Iteration. *Ieee Signal Processing Letters*, *1*(10), 144-146. http://doi.org/10.1109/97.329844

Kay, A. L., Bell, V. A., Guillod, B. P., Jones, R. G., & Rudd, A. C. (2018). National-scale analysis of low flow frequency: historical trends and potential future changes. *Climatic Change*, *147*(3-4), 585-599. http://doi.org/10.1007/s10584-018-2145-y

Krysanova, V., Vetter, T., Eisner, S., Huang, S. C., Pechlivanidis, I., Strauch, M., et al. (2017). Intercomparison of regional-scale hydrological models and climate change impacts projected for 12 large river basins worldwide-a synthesis. *Environmental Research Letters*, 12(10), 105002. http://doi.org/10.1088/1748-9326/aa8359

Lange, S. (2018). Bias correction of surface downwelling longwave and shortwave radiation for the EWEMBI dataset. *Earth System Dynamics*, *9*(2), 627-645. http://doi.org/10.5194/esd-9-627-2018

Leng, G. Y., Tang, Q. H., Huang, M. Y., Hong, Y., & Ruby, L. L. (2015). Projected changes in mean and interannual variability of surface water over continental China. *Science China-Earth Sciences*, *58*(5), 739-754. http://doi.org/10.1007/s11430-014-4987-0

Leng, G. Y., Tang, Q. H., Huang, S. Z., Zhang, X. J., & Cao, J. J. (2016). Assessments of joint hydrological extreme risks in a warming climate in China. *International Journal of Climatology*, *36*(4), 1632-1642. http://doi.org/10.1002/joc.4447

Li, Y., Piao, S., Li, L. Z. X., Chen, A., Wang, X., Ciais, P., et al. (2018). Divergent hydrological response to large-scale afforestation and vegetation greening in China. *Science Advances*, *4*(5), eaar4182. http://doi.org/10.1126/sciadv.aar4182

Liang, X., Wood, E. F., & Lettenmaier, D. P. (1996). Surface soil moisture parameterization of the VIC-2L model: Evaluation and modification. *Global and Planetary Change*, *13*(1-4), 195-206. http://doi.org/10.1016/0921-8181(95)00046-1

Liang, X., Lettenmaier, D. P., Wood, E. F., & Burges, S. J. (1994). A simple hydrologically based model of land surface water and energy fluxes for general circulation models. *Journal of Geophysical Research-Atmospheres*, *99*(D7), 14415-14428. http://doi.org/10.1029/94jd00483

Liu, W., Sun, F., Lim, W. H., Zhang, J., Wang, H., Shiogama, H., & Zhang, Y. (2018). Global drought and severe drought-affected populations in 1.5 and 2℃ warmer worlds. *Earth System Dynamics*, *9*(1), 267-283. http://doi.org/10.5194/esd-9-267-2018

Liu, W., Lim, W. H., Sun, F., Mitchell, D., Wang, H., Chen, D., et al. (2018). Global Freshwater Availability Below Normal Conditions and Population Impact Under 1.5 and 2℃ Stabilization Scenarios. *Geophysical Research Letters*, *45*(18), 9803-9813. http://doi.org/10.1029/2018gl078789

Liu, Y. L., Hejazi, M., Li, H. Y., Zhang, X. S., & Leng, G. Y. (2018). A hydrological emulator for global applications - HE v1.0.0. *Geoscientific Model Development*, *11*(3), 1077-1092.

http://doi.org/10.5194/gmd-11-1077-2018

Lohmann, D., Nolte-Holube, R., & Raschke, E. (1996). A large-scale horizontal routing model to be coupled to land surface parametrization schemes. *Tellus A: Dynamic Meteorology and Oceanography*, *48*(5), 708-721. http://doi.org/ 10.3402/tellusa.v48i5.12200

Lohmann, D., Raschke, E., Nijssen, B., & Lettenmaier, D. P. (1998a). Regional scale hydrology: I. Formulation of the VIC-2L model coupled to a routing model. *Hydrological Sciences Journal-Journal Des Sciences Hydrologiques*, *43*(1), 131-141. http://doi.org/10.1080/02626669809492107

Lohmann, D., Raschke, E., Nijssen, B., & Lettenmaier, D. P. (1998b). Regional scale hydrology: II. Application of the VIC-2L model to the Weser River, Germany. *Hydrological Sciences Journal-Journal Des Sciences Hydrologiques*, *43*(1), 143-158. http://doi.org/10.1080/02626669809492108

Lutz, A. F., ter Maat, H. W., Biemans, H., Shrestha, A. B., Wester, P., & Immerzeel, W. W. (2016). Selecting representative climate models for climate change impact studies: an advanced envelope-based selection approach. *International Journal of Climatology*, *36*(12), 3988-4005. http://doi.org/10.1002/joc.4608

Müller Schmied, H., Adam, L., Eisner, S., Fink, G., Flörke, M., Kim, H., et al. (2016). Variations of global and continental water balance components as impacted by climate forcing uncertainty and human water use. *Hydrology and Earth System Sciences*, *20*(7), 2877-2898. http://doi.org/10.5194/hess-20-2877-2016

Milly, P. C. D., Dunne, K. A., & Vecchia, A. V. (2005). Global pattern of trends in streamflow and water availability in a changing climate. *Nature*, *438*(7066), 347-350. http://doi.org/10.1038/nature04312

Mitchell, D., James, R., Forster, P. M., Betts, R. A., Shiogama, H., & Allen, M. (2016). Realizing the impacts of a 1.5°C warmer world. *Nature Climate Change*, *6*(8), 735-737. https://doi.org/10.1038/nclimate3055

Mitchell, D., AchutaRao, K., Allen, M., Bethke, I., Beyerle, U., Ciavarella, A., et al. (2017). Half a degree additional warming, prognosis and projected impacts (HAPPI): background and experimental design. *Geoscientific Model Development*, *10*(2), 571-583. http://doi.org/10.5194/gmd-10-571-2017

Nangombe, S., Zhou, T., Zhang, W., Wu, B., Hu, S., Zou, L., & Li, D. (2018). Record-breaking climate extremes in Africa under stabilized 1.5°C and 2°C global warming scenarios. *Nature Climate Change*, *8*(5), 375-380. http://doi.org/10.1038/s41558-018-0145-6

Nijssen, B., Schnur, R., & Lettenmaier, D. P. (2001). Global retrospective estimation of soil moisture using the variable infiltration capacity land surface model, 1980-93. *Journal of Climate*, *14*(8), 1790-1808.

http://doi.org/10.1175/1520-0442(2001)014<1790:greosm>2.0.co;2

Nijssen, B., O'Donnell, G. M., Lettenmaier, D. P., Lohmann, D., & Wood, E. F. (2001). Predicting the discharge of global rivers. *Journal of Climate*, *14*(15), 3307-3323. http://doi.org/10.1175/1520-0442(2001)014<3307:ptdogr>2.0.co;2

O'Gorman, P. A., & Schneider, T. (2009). The physical basis for increases in precipitation extremes in simulations of 21st-century climate change. *Proceedings of the National Academy of Sciences of the United States of America*, *106*(35), 14773-14777. http://doi.org/10.1073/pnas.0907610106

O'Neill, B. C., Kriegler, E., Ebi, K. L., Kemp-Benedict, E., Riahi, K., Rothman, D. S., et al. (2017). The roads ahead: Narratives for shared socioeconomic pathways describing world futures in the 21st century. *Global Environmental Change-Human and Policy Dimensions*, *42*, 169-180. http://doi.org/10.1016/j.gloenvcha.2015.01.004

Ouyang, Z., Zheng, H., Xiao, Y., Polasky, S., Liu, J., Xu, W., et al. (2016). Improvements in ecosystem services from investments in natural capital. *Science*, *352*(6292), 1455-1459. http://doi.org/10.1126/science.aaf2295

Piao, S., Friedlingstein, P., Ciais, P., de Noblet-Ducoudré, N., Labat, D., & Zaehle, S. (2007). Changes in climate and land use have a larger direct impact than rising CO_2 on global river runoff trends. *Proceedings of the National Academy of Sciences of the United States of America*, *104*(39), 15242-15247. http://doi.org/10.1073/pnas.0707213104

Prudhomme, C., Giuntoli, I., Robinson, E. L., Clark, D. B., Arnell, N. W., Dankers, R., et al. (2014). Hydrological droughts in the 21st century, hotspots and uncertainties from a global multimodel ensemble experiment. *Proceedings of the National Academy of Sciences of the United States of America*, *111*(9), 3262-3267. http://doi.org/10.1073/pnas.1222473110

Rosenzweig, C., Elliott, J., Deryng, D., Ruane, A. C., Müller, C., Arneth, A., et al. (2014). Assessing agricultural risks of climate change in the 21st century in a global gridded crop model intercomparison. *Proceedings of the National Academy of Sciences of the United States of America*, *111*(9), 3268-3273. http://doi.org/10.1073/pnas.1222463110

Schewe, J., Heinke, J., Gerten, D., Haddeland, I., Arnell, N. W., Clark, D. B., et al. (2014). Multimodel assessment of water scarcity under climate change. *Proceedings of the National Academy of Sciences of the United States of America*, *111*(9), 3245-3250. http://doi.org/10.1073/pnas.1222460110

Schleussner, C.-F., Rogelj, J., Schaeffer, M., Lissner, T., Licker, R., Fischer, E. M., et al. (2016). Science and policy characteristics of the Paris Agreement temperature goal. *Nature Climate Change*, *6*(9), 827-835. http://doi.org/10.1038/nclimate3096

Sharma, A., Wasko, C., & Lettenmaier, D. P. (2018). If Precipitation Extremes Are Increasing, Why Aren't Floods? *Water Resources Research*, *54*(11), 8545-8551. http://doi.org/10.1029/2018wr023749

She, D. X., Xia, J., Shao, Q. X., Taylor, J. A., Zhang, L. P., Zhang, X., et al. (2017). Advanced investigation on the change in the streamflow into the water source of the middle route of China's water diversion project. *Journal of Geophysical Research-Atmospheres*, *122*(13), 6950-6961. http://doi.org/10.1002/2016jd025702

Su, B., Huang, J., Fischer, T., Wang, Y., Kundzewicz, Z. W., Zhai, J., et al. (2018). Drought losses in China might double between the 1.5°C and 2.0°C warming. *Proceedings of the National Academy of Sciences of the United States of America*, *115*(42), 10600-10605. http://doi.org/10.1073/pnas.1802129115

Sun, Q. H., Miao, C. Y., Hanel, M., Borthwick, A. G. L., Duan, Q. Y., Ji, D. Y., & Li, H. (2019). Global heat stress on health, wildfires, and agricultural crops under different levels of climate warming. *Environment International*, *128*, 125-136. http://doi.org/10.1016/j.envint.2019.04.025

Tao, F. L., & Zhang, Z. (2011). Impacts of climate change as a function of global mean temperature: maize productivity and water use in China. *Climatic Change*, *105*(3-4), 409-432. http://doi.org/10.1007/s10584-010-9883-9

Todini, E. (1996). The ARNO rainfall-runoff model. *Journal of Hydrology*, *175*(1-4), 339-382. http://doi.org/10.1016/s0022-1694(96)80016-3

Trenberth, K. E. (2011). Changes in precipitation with climate change. *Climate Research*, *47*(1-2), 123-138. http://doi.org/10.3354/cr00953

UNFCCC. (2015). Adoption of the Paris Agreement, paper presented at Conference of the Parties, Paris, France, 30 November–11 December, 2015.

van Vliet, M. T. H., Franssen, W. H. P., Yearsley, J. R., Ludwig, F., Haddeland, I., Lettenmaier, D. P., & Kabat, P. (2013). Global river discharge and water temperature under climate change. *Global Environmental Change-Human and Policy Dimensions*, *23*(2), 450-464. http://doi.org/10.1016/j.gloenvcha.2012.11.002

Wang, H. M., Chen, J., Cannon, A. J., Xu, C. Y., & Chen, H. (2018). Transferability of climate simulation

uncertainty to hydrological impacts. *Hydrology and Earth System Sciences*, *22*(7), 3739-3759. http://doi.org/10.5194/hess-22-3739-2018

Wasko, C., & Sharma, A. (2017). Global assessment of flood and storm extremes with increased temperatures. *Scientific Reports*, *7*, *7945*. http://doi.org/10.1038/s41598-017-08481-1

Weedon, G. P., Gomes, S., Viterbo, P., Shuttleworth, W. J., Blyth, E., Österle, H., et al. (2011). Creation of the WATCH Forcing Data and Its Use to Assess Global and Regional Reference Crop Evaporation over Land during the Twentieth Century. *Journal of Hydrometeorology*, *12*(5), 823-848. http://doi.org/10.1175/2011jhm1369.1

Woldemeskel, F. M., Sharma, A., Sivakumar, B., & Mehrotra, R. (2014). A framework to quantify GCM uncertainties for use in impact assessment studies. *Journal of Hydrology*, *519*, 1453-1465. http://doi.org/10.1016/j.jhydrol.2014.09.025

Wu, H., Kimball, J. S., Mantua, N., & Stanford, J. (2011). Automated upscaling of river networks for macroscale hydrological modeling. *Water Resources Research*, *47(3)*, *W03517*. http://doi.org/10.1029/2009wr008871

Xu, W., Xiao, Y., Zhang, J., Yang, W., Zhang, L., Hull, V., et al. (2017). Strengthening protected areas for biodiversity and ecosystem services in China. *Proceedings of the National Academy of Sciences of the United States of America*, *114*(7), 1601-1606. http://doi.org/10.1073/pnas.1620503114

Yin, J. B., Gentine, P., Zhou, S., Sullivan, S. C., Wang, R., Zhang, Y., & Guo, S. L. (2018). Large increase in global storm runoff extremes driven by climate and anthropogenic changes. *Nature Communications*, *9*, *4389*. http://doi.org/10.1038/s41467-018-06765-2

Zhai, R., Tao, F., & Xu, Z. (2018). Spatial-temporal changes in runoff and terrestrial ecosystem water retention under 1.5 and 2°C warming scenarios across China. *Earth System Dynamics*, *9*(2), 717-738. http://doi.org/10.5194/esd-9-717-2018

Zhou, T., Nijssen, B., Gao, H. L., & Lettenmaier, D. P. (2016). The Contribution of Reservoirs to Global Land Surface Water Storage Variations. *Journal of Hydrometeorology*, *17*(1), 309-325. http://doi.org/10.1175/jhm-d-15-0002.1

Table 1. Selected countries according to population and GDP data under baseline period.

The top 20 countries in the world according to population
China (CHN); India (IND); United States of America (USA); Indonesia (IDN); Brazil (BRA); Pakistan (PAK); Russian Federation (RUS); Nigeria (NGA); Bangladesh (BGD); Japan (JPN); Mexico (MEX); Philippines (PHL); Viet Nam (VNM); Germany (DEU); Ethiopia (ETH); Egypt (EGY); Turkey (TUR); Iran (Islamic Republic of; IRN); Thailand (THA); France (FRA)
The top 20 countries in the world according to GDP
United States of America (USA), China (CHN), Japan (JPN), India (IND), Germany (DEU), United Kingdom of Great Britain and Northern Ireland (GBR), France (FRA), Russian Federation (RUS), Italy (ITA), Brazil (BRA), Mexico (MEX), Spain (ESP), Korea (the Republic of; KOR), Canada (CAN), Iran (Islamic Republic of; IRN), Indonesia (IDN), Turkey (TUR), Australia (AUS), Saudi Arabia (SAU), Netherlands (NLD)

* Country names are displayed in ISO3 format

Table 2. Percentage of population which would be influenced by extreme low runoff decrease, extreme high runoff increase, extreme low runoff decrease and extreme high runoff increase concurrently in different continents and over the world.

Influenced population	Africa		Asia		Europe		North America		Oceania		South America		World	
	1.5 ℃	2.0 ℃	1.5 ℃	2.0 ℃	1.5 ℃	2.0 ℃	1.5 ℃	2.0 ℃	1.5 ℃	2.0 ℃	1.5 ℃	2.0 ℃	1.5 ℃	2.0 ℃
Extreme low runoff decrease	51.2 %	44. 4%	35. 9%	38. 2%	53. 5%	73. 5%	43. 3%	54. 6%	45.8 %	37. 6%	81. 2%	62. 1%	44. 6%	45. 1%
Extreme high runoff increase	34.8 %	51. 0%	74. 9%	79. 5%	49. 7%	43. 1%	46. 3%	17. 6%	7.0 %	24. 3%	30. 1%	40. 6%	56. 1%	61. 0%
Extreme low runoff decrease and extreme high runoff increase	5.8 %	13. 1%	20. 7%	27. 2%	17. 4%	21. 2%	13. 7%	7.4 %	3.6 %	6.5 %	21. 5%	17. 0%	15. 3%	20. 2%

* Greenland and grid cells with annual runoff < 5 mm in the baseline period are masked.

Table 3. Percentage of GDP which would be influenced by extreme low runoff decrease, extreme high runoff increase, extreme low runoff decrease and extreme high runoff increase concurrently in different continents and over the world.

Influenced GDP	Africa		Asia		Europe		North America		Oceania		South America		World	
	1.5℃	2.0 ℃	1.5 ℃	2.0 ℃	1.5 ℃	2.0 ℃	1.5 ℃	2.0 ℃	1.5 ℃	2.0 ℃	1.5 ℃	2.0 ℃	1.5 ℃	2.0 ℃
Extreme low runoff decrease	46.5 %	44. 3%	36. 8%	41. 0%	50.2 %	75. 2%	42. 7%	54.4 %	40.0 %	30. 1%	82.5 %	63.5 %	43. 7%	48. 3%
Extreme high runoff increase	35.9 %	50. 1%	75. 6%	80. 9%	49.4 %	43. 1%	47. 7%	19.1 %	4.6 %	20. 4%	30.8 %	40.9 %	57. 1%	59. 5%
Extreme low runoff decrease and extreme	5.4%	13. 5%	21. 5%	30. 0%	15.3 %	23. 2%	15. 3%	8.5 %	1.7 %	4.2 %	22.5 %	17.0 %	16. 2%	21. 9%

high runoff increase

* Greenland and grid cells with annual runoff < 5 mm in the baseline period are masked

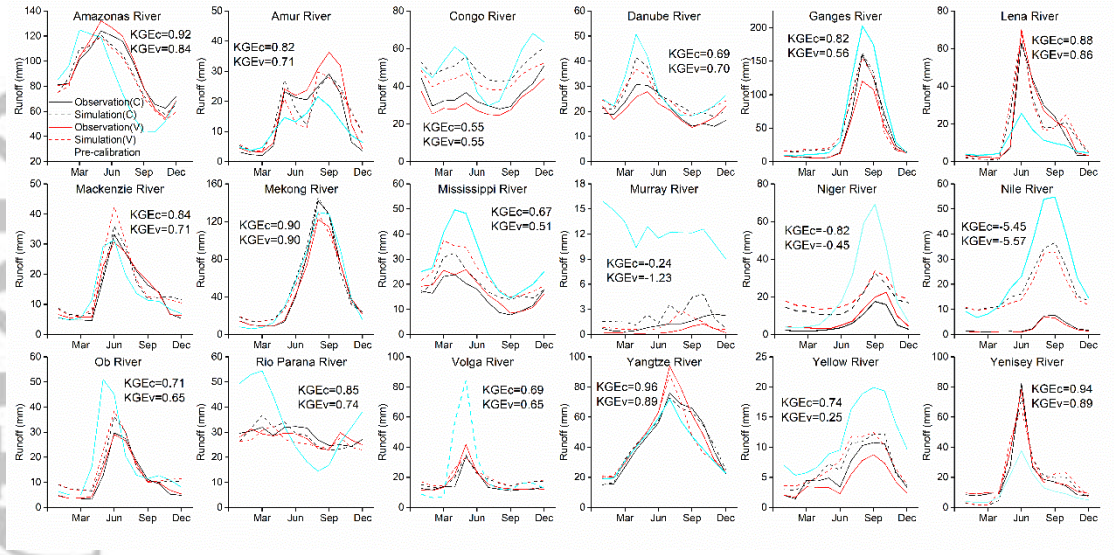

Figure 1. Observed (solid lines) and simulated (dashed lines) monthly runoff (mm) during the calibration period (black lines) and validation period (red lines) aggregated to the basin level at specific gauge stations (Table S1) in all 18 basins considered in this study. Blue lines represent uncalibrated results. C and V represent calibration period and validation period, respectively.

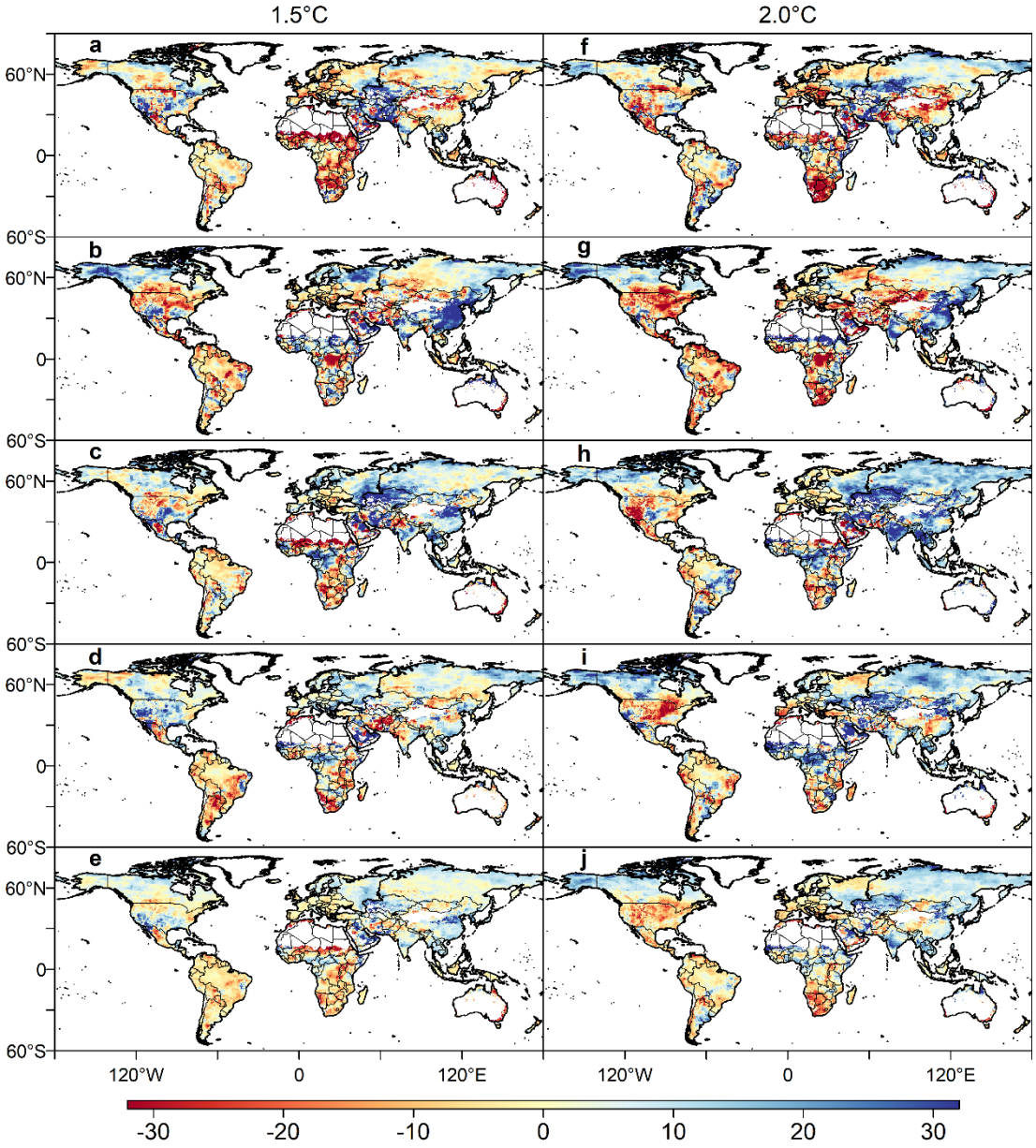

Figure 2. Median values of the projected changes in annual runoff (%) over the world under the 1.5°C (a-e) and 2.0°C (f-j) warming scenarios by ECHAM6-3-LR (a,f), MIROC5 (b, g), NorESM1-HAPPI (c,h), CAM4-2degree (d,i), and all four GCMs (e,j), relative to 2006-2015. Greenland and grid cells with annual runoff < 5 mm in the baseline period are masked.

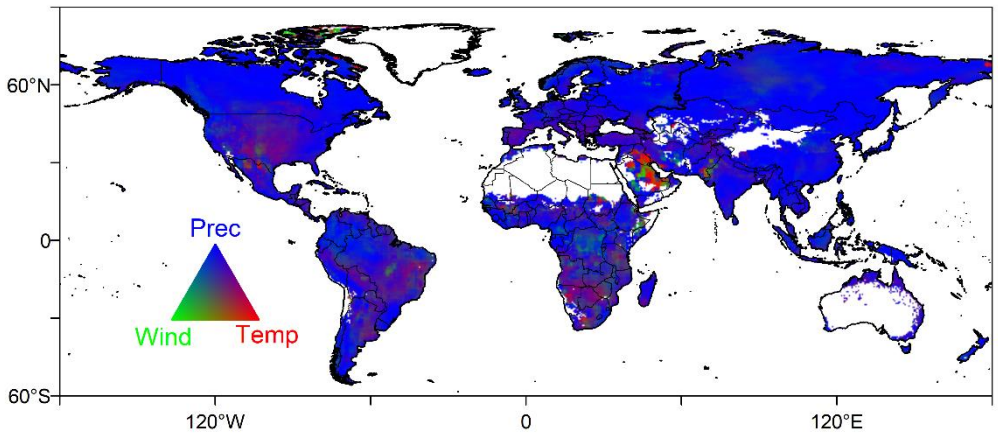

Figure 3. The weight of the three key factors in which Prec, Temp, Wind represent annual precipitation change, annual mean temperature change and annual mean wind speed change, based on the coefficient of determination (r^2) between each predictor change to annual runoff change. Greenland and grid cells with annual runoff < 5 mm in the baseline period are masked.

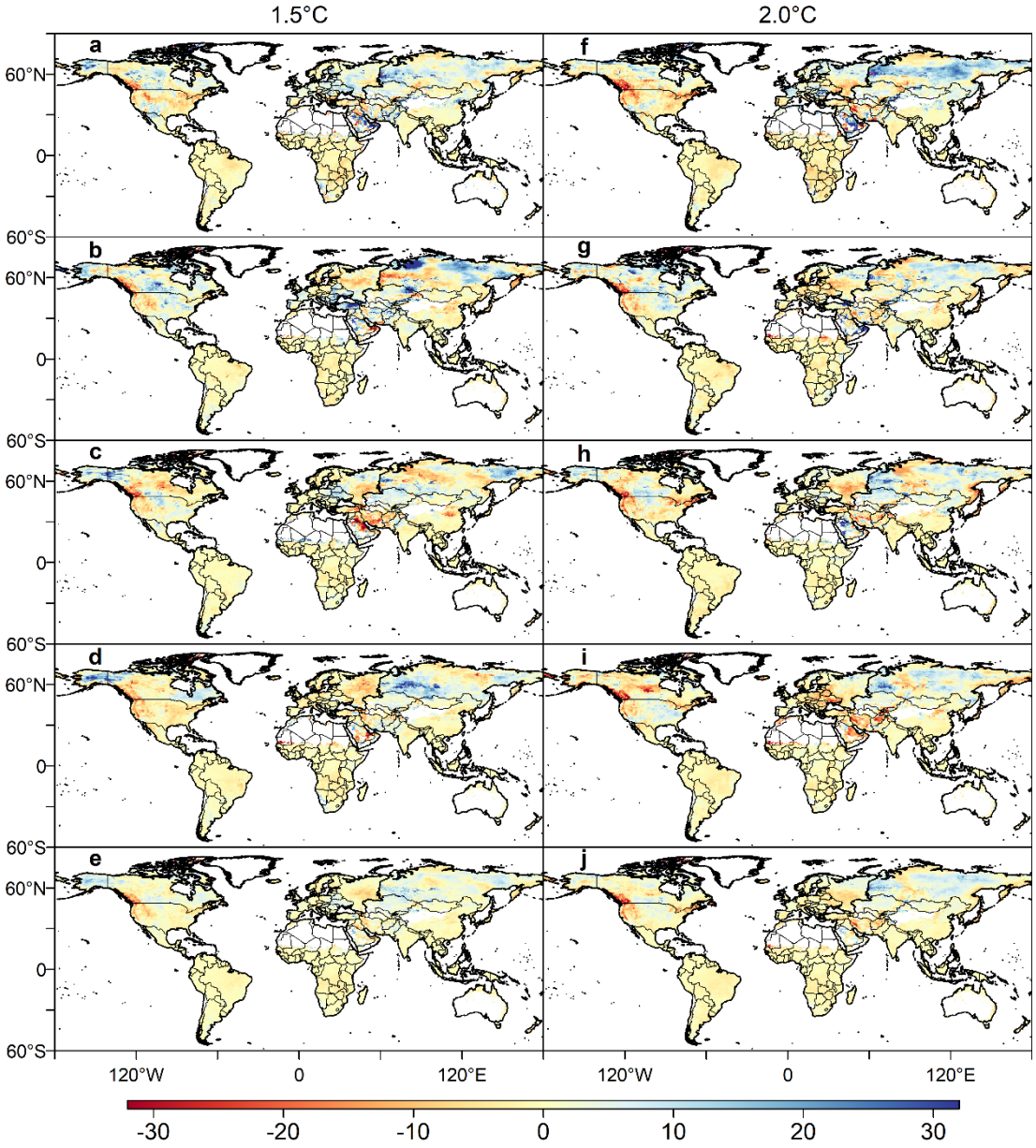

Figure 4. Median values of the projected changes (%) in annual TEWR over the world under the 1.5°C (a-e) and 2.0°C (f-j) warming scenarios by ECHAM6-3-LR (a,f), MIROC5 (b, g), NorESM1-HAPPI (c,h), CAM4-2degree (d,i), and all four GCMs (e,j), relative to 2006-2015. Greenland and grid cells with annual runoff < 5 mm in the baseline period are masked.

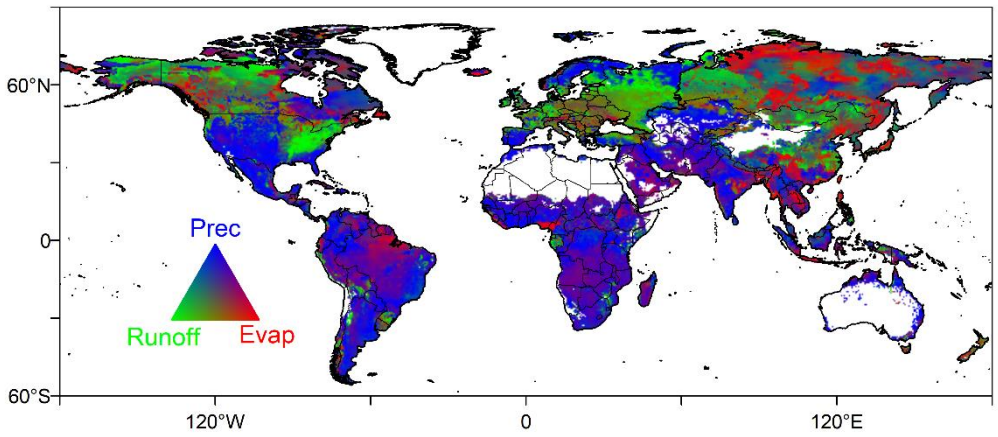

Figure 5. The weight of the three key factors in which Prec, Evap, Runoff represent annual precipitation change, annual evapotranspiration change and annual runoff change, based on the coefficient of determination (r^2) between each predictor to annual TEWR change. Greenland and grid cells with annual runoff < 5 mm in the baseline period are masked.

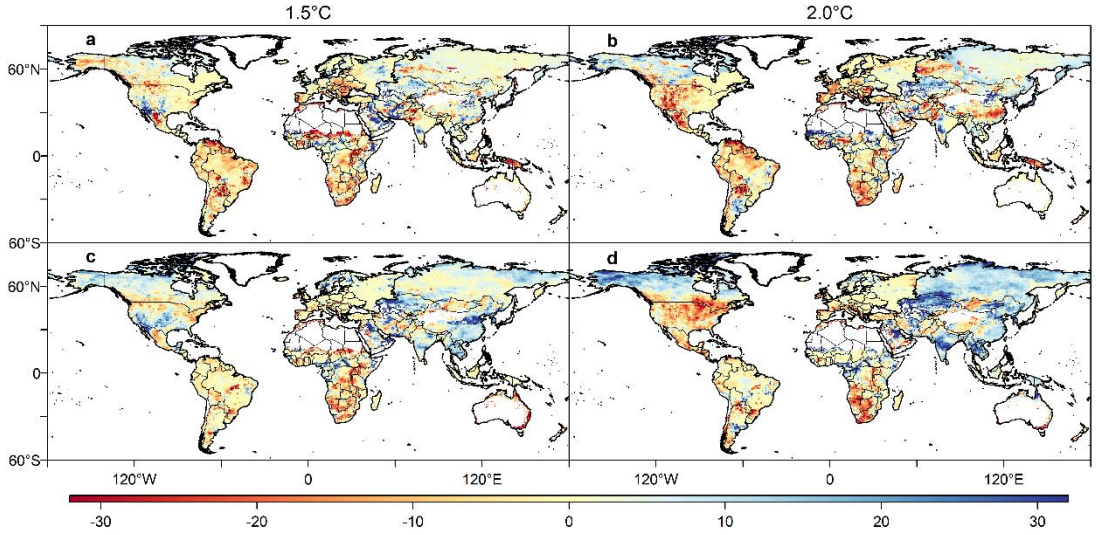

Figure 6. Changing trends of extreme low runoff (a,b) and extreme high runoff (c,d) under 1.5 (a,c) and 2.0°C (b,d) warming scenarios (2106-2115) relative to the baseline period (2006-2015). Greenland and grid cells with annual runoff < 5 mm in the baseline period are masked.

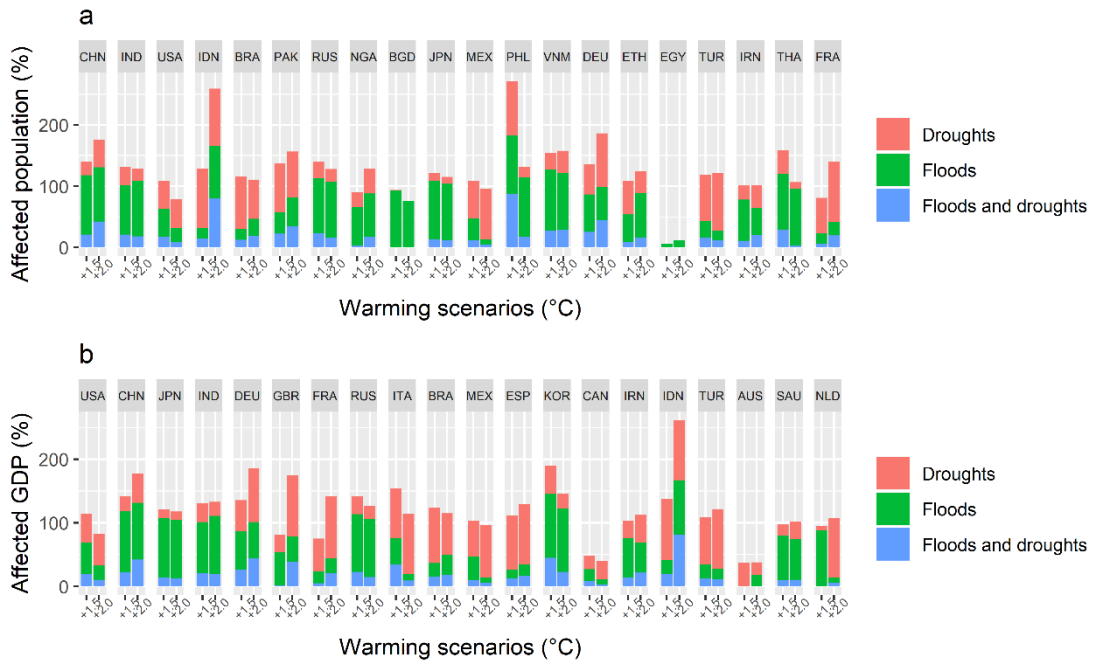

Figure 7. Stacked bar about proportion of affected population (a) and GDP (b) under 1.5 and 2.0°C warming scenarios in the top 20 countries, respectively. The red, green, blue parts represent proportion of population or GDP would potentially be affected by droughts, floods, droughts and floods, respectively. Country names are displayed in ISO3 format, full names are listed in Table 1. Greenland and grid cells with annual runoff < 5 mm in the baseline period are masked.

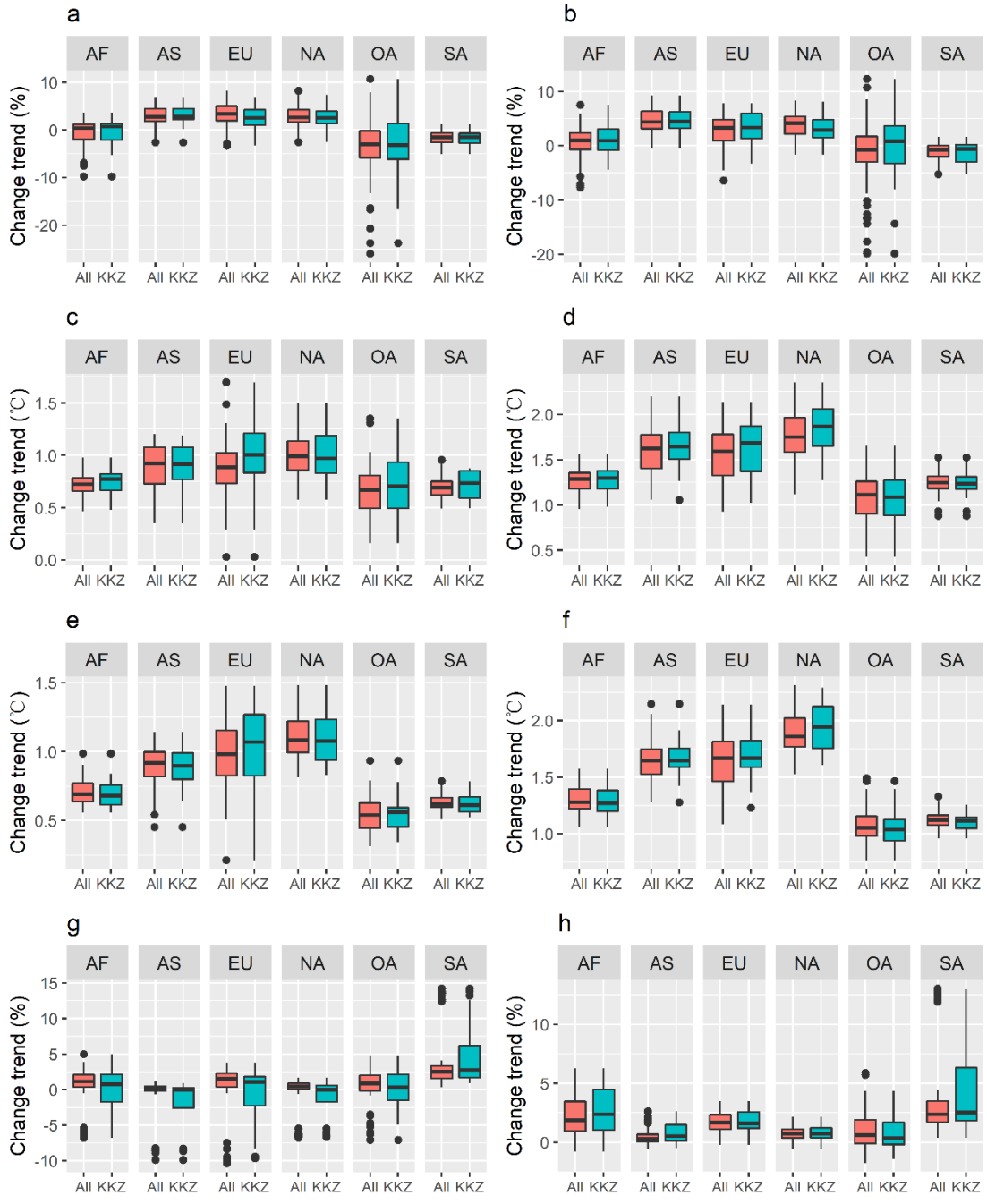

Figure 8. Changes in area-weighted average precipitation (a,b), maximum temperature (c,d), minimum temperature (e,f), wind speed (g,h) at continental scale (AF: Africa; AS: Asia; EU: Europe; NA: North America; OA: Oceania; SA: South America) among all 70 ensembles (3 GCMs × 20 ensembles +1 GCM × 10 ensembles; All) and 20 ensembles (4 GCMs × 5 ensembles; KKZ) selected through KKZ method under 1.5 (a,c,e,g) and 2.0°C (b,d,f,h) warming scenarios.